Process Safety and Environmental Protection 147 (2021) 1077–1087

Contents lists available at ScienceDirect

Process Safety and Environmental Protection

journal homepage: www.elsevier.com/locate/psep

Potassium struvite (slow release fertilizer) and activated carbon production: Resource recovery from vinasse and grape marc organic waste using thermal processing

Hasan Arslanoğlu[a,*], Fikret Tümen[b]

[a] Kırşehir Ahi Evran University, Faculty of Engineering and Architecture, Department of Chemical and Process Engineering, 40200, Kırşehir, Turkey
[b] Department of Chemical Engineering, Firat University, 23200, Elazig, Turkey

ARTICLE INFO

Article history:
Received 18 September 2020
Received in revised form 14 January 2021
Accepted 16 January 2021
Available online 23 January 2021

Keywords:
Vinasse
Grape marc
Pyrolysis
Potassium-struvite
Slow-release fertilizer
Activated carbon
Circular economy

ABSTRACT

This study investigated the production conditions of a potassium magnesium phosphate fertilizer with vinasse (a by-product of the sugar or ethanol industry) and grape marc (a by-product of the wine-making industry). A mixture of vinasse and grape marc was subjected to pyrolysis under a nitrogen gas atmosphere, and water was used to extract potassium from the end product. Potassium magnesium phosphate (potassium-struvite, $KMgPO_4.6H_2O$), a slow-release fertilizer compound, was obtained from the extract with potassium to explore process conditions and product characteristics. Producing fertilizer products from residual materials is of paramount significance for conserving natural resources. The mixture was pyrolyzed, allowing us to remove potassium from the complex matrix of concentrated vinasse to a clear and high alkaline solution. The residual carbon was activated by decomposing (pyrolysis) and treating the residue and then washing it with water. The extract had high alkalinity, suggesting that the potassium in the mixture resulted in carbon activation during biomass pyrolysis. Pyrolysis and treatment can be used to produce activated carbon from vinasse. This study also investigated the solubility of vinasse in water and aqueous solutions. K-struvite with 10.67 % K_2O was about 2% soluble in water, indicating that the end product was a slow-release fertilizer agent. In conclusion, this process can be used to produce potassium (a slow-release fertilizer) and activated carbon (a by-product) from vinasse for different purposes.

1. Introduction

Vinasse (stylage) is a by-product of the sugar or ethanol industry. The greatest challenge faced by molasses-based alcohol factories is how to reuse the vinasse. One liter of alcohol results in about 12–15 liters of vinasse (Reis et al., 2019; Arslanoğlu et al., 2020; Liang et al., 2012). The disposal of slurry with high organic matter causes water contamination. Therefore, some alcohol factories in Turkey have been forced to halt production. The properties - and thus recycling potential - of vinasse depend on the type of material (molasses, corn, potato, etc.) from which alcohol is produced. Molasses are used as a supplement to livestock meals because it contains a high amount of salt. The best way to use vinasse is as a fertilizer in yeast production. However, only a few facilities prepare mash from vinasse (Arslanoğlu et al., 2020; Liang et al., 2012). It is hard to transport a large amount of dilute slurry (8–10 Bx) as a fertilizer. Vinasse used to be discharged directly into natural waterways, causing environmental pollution (60,000−70,000 mg/L COD and 25,000−30,000 mg/L BOD). However, today it is converted into valuable products, such as a liquid fertilizer with potassium sulfate (Liang et al., 2012; Barampouti et al., 2019; Li and Mupondwa, 2018). Scientists hold anthropological factors and chemical fertilizers responsible for eutrophication in water bodies, suggesting that we should use fertilizers more carefully for both environmental and economic sustainability. Therefore, slow-release fertilizers have been of great interest in recent years.

Mineral fertilizers are mostly highly soluble compounds. However, their discharge to the soil causes losses due to precipitation and washing and drifting during irrigation, resulting in eutrophication in surface waters. Coating methods are used to achieve slow or controlled solubility in mineral fertilizers with sulfur, humic substances, resins, and polymers (Irfan et al., 2018). One way of dissolving fertilizers with nutrients is to use compounds with low solubility. Double phosphates of magnesium, a group of minerals with nutrient elements used by plants, have limited solubility in normal water and soil environments. Ammonium-struvite

* Corresponding author.
E-mail address: hasan.arslanoglu@ahievran.edu.tr (H. Arslanoğlu).

https://doi.org/10.1016/j.psep.2021.01.025
0957-5820/

($MgNH_4PO_4.6H_2O$) is the most popular slow-release fertilizer, and therefore, numerous research has focused on its characteristics and recovery as a by-product from final wastes of treatment systems. There is little research on the characteristics and production of potassium struvite ($MgKPO_4.6H_2O$), although it is an analog of ammonium struvite with valuable nutrients. Potassium struvite is superior to ammonium-struvite because it does not degrade (Salutsky and Steiger, 1964; Chojnacka et al., 2019) or cause ammonia loss observed in urea-based fertilizers after their introduction into the soil. Vinasse-based potassium sulfate is quickly washed away by rain and irrigation water because it is highly soluble in water (120 g/L) (Lide, 1995). On the other hand, $MgKPO_4.6H_2O$ has a solubility of about 0.08 g/L (Yang et al., 2019). One study reported it equal to or higher than 2.0 g/L (Salutsky and Steiger, 1964), while another found it to be lower than 0.2 g/L (Tian et al., 2020).

Turkey has four alcohol factories (Eskisehir, Turhal, Malatya, and Erzurum), producing 60 million liters of ethanol from sugar beet molasses per year. However, only the alcohol factory in Eskisehir operates regularly and has vinasse thickening and potassium sulfate production units. The sugar factory in Amasya is a new private factory with additional facilities capable of producing 60,000 L of alcohol and 110 tons of concentrated vinasse per day. However, those facilities do not operate at maximum capacity. Pankobirlik (Sugarbeet Growers Cooperatives Association) has also established an ethanol plant with an annual capacity of 84 million liters to produce bioethanol, a by-product of sugar beet. The plant produces concentrated and doped concentrate vinasse as a fertilizer (Hidalgo et al., 2019). According to the Official Gazette (No. 28346 & Date: 7, 2012), (1) gasoline delivered by refinery license holders via land tanker filling units and (2) gasoline delivered to dealers by distributor license holders must contain at least 2% ethanol (as of 01.01.2014) and at least 3% ethanol (as of 01.01.2014) (Web-7). With this regulation, the bioethanol mix ratio increased with an increase in the amount of bioethanol consumed in Turkey. With increased bioethanol production, the sugar factories will regularly produce alcohol, increasing the amount of molasses.

Potassium magnesium phosphate (potassium-struvite), a slow-release fertilizer, can be produced from potassium in vinasse. To that end, preliminary studies performed vinasse pyrolysis impregnated with lignocellulosic substances, which was then extracted with water. The results showed that potassium can be extracted into a high-efficiency solution and that the resulting solution is a colorless solution with high alkalinity. Not only does an alkaline medium provide a suitable environment for the precipitation of potassium-struvite, but it also reduces the need to use basic components during precipitation. Grape marc contains some potassium (Patti et al., 2009; Ferjani et al., 2019), and therefore, should be used as a lignocellulosic material in a process within that framework. Turkey is the world's sixth largest grape producer (4.255.000 tons annually) and accounts for 5.8 % of the total grape production worldwide. About 80 percent of the grape harvest worldwide is used to produce wine, while the remaining is disposed of as waste (Lafka et al., 2007; Algieri et al., 2019). However, there is little research in Turkey on the reuse of grape industrial waste.

This study, therefore, designed a three-step process: (1) pyrolysis of a mixture of grape marc and vinasse, (2) extraction of potassium into solution, and (3) precipitation of potassium-struvite. The process was based on the assumption that the post-extraction carbonized material could be converted into activated carbon by superheating it with potassium compounds and that a second product could be obtained to use for water treatment. This study aimed to produce an eco-friendly fertilizer and activated carbon from a grape marc and vinasse mixture. Those products will have added value because they will be economically and environmentally sustainable. We believe that slow- or controlled- release natural fertilizers yield the same output and cause less pollution than commercial fertilizers. In this study, concentrated vinasse and grape marc were mixed and then extracted with water for pyrolysis. Concentrated vinasse was supplied from the Sugar Factory in Eskisehir, while grape marc was supplied from the Eskibaglar Wine Factory in Elazig. Potassium-struvite was precipitated from the extract, and activated carbon was stabilized from the carbonized residue using an acid solution. The resulting products were characterized.

2. Proposed technological concept

Vinasse should not be directly discharged to the environment because it contains a high amount of organic matter. Nitrogen and potassium content is a sign of fertilizer quality. Vinasse is hard to transport because it is very dilute, and therefore, it can be used directly only where it is produced. Besides, its use is limited due to high organic content. Thus, it is concentrated and treated with sulfuric acid to recover its potassium as potassium sulfate in many embodiments. In Turkey, this process is carried out in the alcohol production facilities of sugar factories. However, potassium sulfate production has been halted due to the ease of transporting concentrated vinasse from the factory to the dilute state. Potassium sulfate is a potassium salt used as a fertilizer. However, it cannot be used as widely as fast-release fertilizers because it is highly soluble in water. Vinasse potassium cannot be used as a fertilizer if it is in small concentrations and has poor qualities (e.g., fast-release). This study aimed to obtain a slow-release fertilizer ($KMgPO_4.6H_2O$; potassium magnesium phosphate, potassium-struvite) from vinasse.

First, struvite was precipitated in a concentrated vinasse medium. To that end, a reasonable amount of phosphoric acid and $MgCl_2$ were mixed in a plate with a K: P: Mg ratio of 1:1:1 based on potassium. The pH was then adjusted to 8−10. The whole mass was crystallized, and the excess NaOH solution was spent. The crystals were Na_3PO_4. The same experiments were performed in a more diluted medium. The consumption of NaOH solution was, again, high. A brown/white precipitate was obtained. Weight was calculated in a solid, which was filtered off and dried after washing. Chemical analyses were performed, and XRD diagrams were obtained. The result showed that the end product was an amorphous mass of mostly magnesium and calcium phosphates and little potassium.

A vinasse medium generally contains organic acids and their salts and plant components (betaine, pyrimidine, etc.) and protein components, probably due to excessive buffer and NaOH solution consumption. Therefore, potassium-struvite precipitation in a vinasse medium is not very suitable. Besides, even if a significant amount of potassium is removed from vinasse, the remaining liquid residue contains a high sodium concentration and creates a waste stream, which is unusable and even contains pollutants. Therefore, potassium-struvite was directly precipitated from a concentrated vinasse medium, but vinasse was pyrolyzed by impregning a lignocellulosic agent, i.e., grape marc. Subsequent extraction with water yielded an alkaline medium purified from potassium impurities and taken up in solution with high yield. Precipitation in that medium resulted in more K-struvite. For example, potassium salts resulting from pyrolysis can promote mass activation, and the residue of extracted potassium can be considered activated carbon. Therefore, this study focused on this method (Fig. 1).

3. Materials and methods

3.1. Supply and preparation of vinasse and grape marc

Concentrated vinasse (200 kg) was supplied from the Eskisehir Sugar Factory Alcohol Production Facilities and divided into two

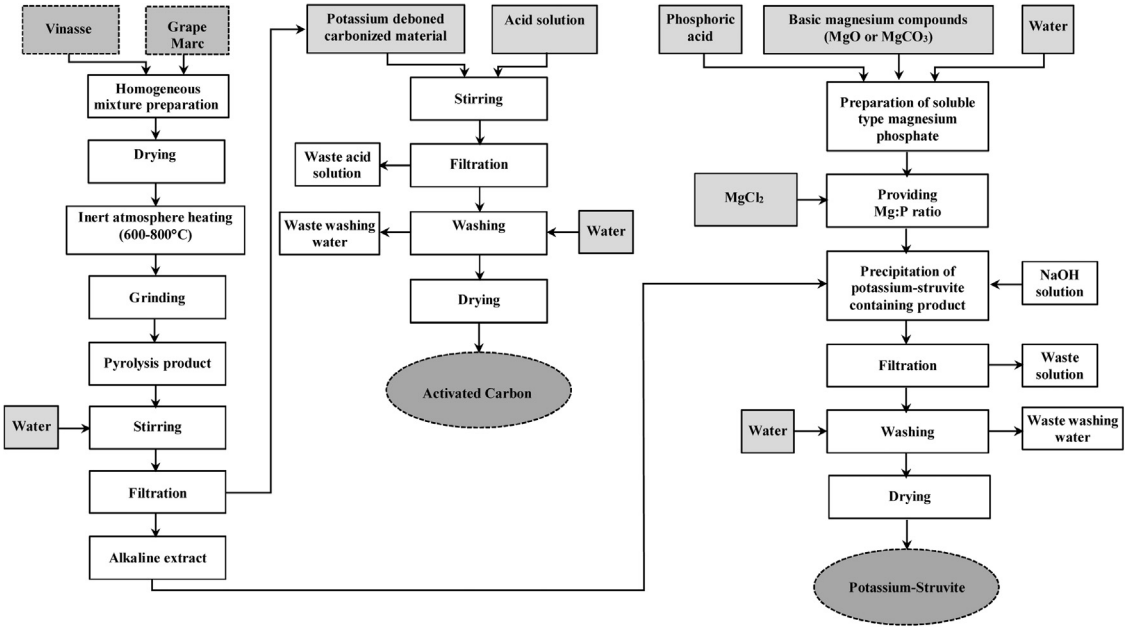

Fig. 1. Flow chart of processes for obtaining potassium-struvite and activated carbon from vinasse and grape marc.

parts. Some were kept in the refrigerator at −16 °C and some at +3 °C. Grape marc was supplied from the Eskibaglar Wine Factory in Sivrice/Elazığ and washed with water on a clean concrete floor. The grape seeds, which contain most of the grape stalk, were dried out in the open and then removed. They were then dried in batches in an oven at 80 °C for 24 h and milled in a Renas Spice-Herb Grinder IC-25B grinder and sieved to -50 mesh (<0.3 mm) size. The samples were kept in closed plastic jars throughout the study (Fig. S1) (Arslanoğlu, 2016; Tümen, 2016).

3.2. Chemicals

The chemicals used in the experiments were supplied from commercially available products of various purity companies. The reactive chemicals used for analysis and analytical purity and standard were certified products.

3.3. Pyrolysis system

The pyrolysis system consisted of a chamber furnace (Protherm PLF 110/15) through which nitrogen gas can pass at a specific flow rate. The temperature of the chamber furnace is computer-controlled. The chamber (22 × 23 × 34) can hold nine pieces of 85 mL crucible at the same time and is equipped with a chimney and aspirator system for the removal of exhaust gases (Fig. 2).

3.4. Pyrolysis and potassium extraction

The samples were stored in an oven at 100 °C for 6–48 h. For pyrolysis, nitrogen gas was first introduced into the chamber at 600 °C and 800 °C at a rate of 300 mL/min for 120 m. Afterward, the samples were placed in the oven at room temperature, and nitrogen gas was introduced for 10 min. The oven reached 600 °C and 800 °C in 15 and 20 min, respectively. Pyrolysis was carried out in a furnace (600 °C and 800 °C) for 120 min. Afterward, the samples were removed from the oven and left to cool down in a vacuum desiccator. The pyrolysis products were milled and sieved through a 200 mesh (<0.075 mm) sieve. The samples were extracted with water under standardized conditions [water/(pyrolysis product) at a ratio of 10, room temperature (23–27 °C) for 120 min, with

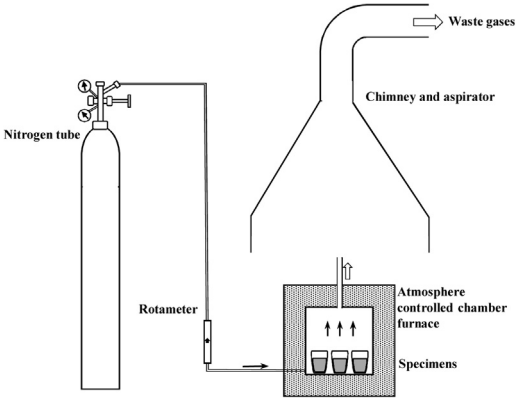

Fig. 2. Pyrolysis system.

shaking at 200 rpm. Por no: 4 Gooch crucible was filtered using a Rocker-300 vacuum pump. The extracts were separated from the solid. pH measurements and K, Na, and Ca and oxidability analyses were performed.

3.5. Activated carbon

The post-extraction solid samples were mixed with 2 M HCl solution (10 times the pyrolysis product from which it was obtained) with agitation for 12 h. The solid separated from the liquid was washed with distilled water until neutrality. The $AgNO_3$ solution of the elution samples did not form AgCl, and the resulting solid was dried at 100 °C for 12 h. Afterward, BET surface area measurements, tests, and analyses were performed.

3.6. Precipitation of potassium-struvite from pyrolysis product extract

First, a potassium-containing extract was obtained from the pyrolysis product according to the procedure (Flow Chart in Fig. S2) involving two steps of extraction using (1) 10 g of pyrolysis product and (2) 100 mL of water. About 50 L of the extract was obtained. Solution composition was determined. A portion of the

extract was concentrated by evaporation. The concentrated extract containing about 2 M K^+ was stored for experiments.

The principle reaction to obtain potassium struvite is as follows:

$$K^+ + Mg^{2+} + PO_4^{3-} + 6H_2O \rightarrow KMgPO_4.6H_2O \quad (1)$$

The following procedure was used to precipitate potassium-struvite. Different final pHs were obtained after adding K, Mg, and P (ratio of 1:1:1) to the intermediate product with H_3PO_4-$MgCO_3$-$MgCl_2.6H_2O$ and 2 N NaOH solution to the mixture. The precipitates were obtained as described above, and analyses were performed on the dried samples. Structural and chemical analyses were performed.

3.7. Solubility tests on potassium-struvite

The decomposition of acids and organic substances secreted by plant roots results in humic and fulvic substances. The solutions of those substances can dissolve slow-release fertilizer components. Therefore, the dissolution of a product with potassium struvite in mineral acid (HCl), citric acid, formic acid, acetic acid, oxalic acid, humic acid, ammonium citrate, ammonium oxalate, ammonium acetate, DTPA, and EDTA solutions was determined. The K:Mg:P ratio was adjusted to 1:1:1, and the pH was adjusted to 9.5 with NaOH solution to precipitate potassium-struvite. This product was used in solubility tests performed in various media. To that end, the potassium-struvite-containing product obtained by drying at 40 °C was stirred at room temperature (23–27 °C) in a 0.001 M solution of the above substances in a solid/liquid ratio of 10 g/L. To do that, 0.4 g of solid was weighed in a 50 mL Falkon tube, and 40 mL of solution was added. The mouth was tightly closed, and 16 tubes were placed in an end-over-end rotator (Dragonlab, MX-RL-Pro). The mixtures were stirred at 50 rpm for one day, and then, the tubes were centrifuged at 6500 rpm for ten min. pH measurements and potassium, phosphorus, and magnesium analyses were performed.

3.8. Instruments and measurements

Potassium-struvite characterization was performed using proximate and ultimate analysis, X-ray diffraction (XRD, Rigaku D-max-2200), particle size distribution (Malvern Master Sizer 3000), FT-IR (Perkin Elmer Spectrum 100), TGA-DTA (FEI Quanta 250 FEG), and SEM-EDX (Jeol JSM-7001 F) analysis. The activated carbon was examined using elemental analysis (LECO CHNS 932 Elemental Analyzer), SEM-EDX (FEI Quanta 250 FEG), X-ray diffraction (XRD, Rigaku D-max-2200), BET surface area (Micromeritics ASAP 2020), pH_{zpc} (Malvern Nanosize ZS-3600 Zetasizer ash content in terms of ASTM D3174-73, iodine number analysis by the sodium thiosulfate volumetric method (ASTM D 4607-94), and functional group analysis by Boehm's titration (Boehm, 1994, 2002).

4. Results and discussion

4.1. Properties of vinasse and grape marc

Tables 1 and S1 show the analysis results for the concentrated vinasse. Tables 2 and S2 show the analysis results for the grape marc. The vinasse and grape marc were used for pyrolysis experiments.

4.2. Pyrolysis experiments and mechanism

Pyrolysis decomposes potassium and sodium compounds into oxides and carbonates and reduces them to a metallic state, and forms various gases (H_2, CO_2, CO, N_2, H_2O) during all those degradation reactions. Porosity, and hence, surface increases in the mass with gases separating from the mass and entering and exiting the metallic components in the carbon mesh (Alcañiz-Monge and Illán-Gómez, 2008; Sevilla and Fuertes, 2013). Alkali carbonate, oxide, and metals form during washing with water after hydration, dissolution, and hydrolysis, followed by the separation of carbon mesh from cavities. Consequently, the surface of the remaining mass causes further expansion. The high pH of the water extract indicated that those events took place, the chemical reaction equations of which are as follows (Arslanoğlu, 2019):

During pyrolysis:

$$(C, H, O, N) + Me\ (K \text{ and } Na) \rightarrow Me_2CO_3 + C + CO \uparrow$$
$$+CO_2 \uparrow + H_2O \uparrow + H_2 \uparrow + N_2 \uparrow$$

The products may also contain large molecular tarry substances due to degradation and coupling reactions. Other hypothetical events are as follows:

$$Me_2CO_3 \rightarrow Me_2O + CO_2 \uparrow$$

$$Me_2O + C \rightarrow 2Me + CO \uparrow$$

Table 1
Some properties of concentrated vinasse.

Properties	Value
Density (g/cm^3)	1.31
pH[a]	5.3
Conductivity (μs/cm) (×1000)[b]	332
Turbidity (NTU) (×1000)[b]	29.8
Heating Loss at 600 °C (%)[c]	50.32
Ash (in 950 °C) (%)[d]	9.9
COD (mg-O_2/l)[b]	571,000
Color (Absorbans)[e]	116 / 39 / 17
Viscosity (cP)	936
Dry Matter (Bx)	63.5
Total Nitrogen (mg-N/ kg)[f]	28,600
Phosphorus (mg/kg)[f]	207
Potassium (mg/kg)[f]	66,500
Sodium (mg/kg)[f]	14,900
Calcium (mg/kg)[f]	3800
Magnesium (mg/kg)[f]	565

[a] Measurements in medium obtained by diluting the concentrated vinasse five times.
[b] Measurements in medium obtained by diluting the concentrated vinasse thousand times.
[c] Constant weighing result at 600 °C. [d] Constant weighing result at 950 °C.
[e] Measurements in medium obtained by diluting the concentrated vinasse thousand times (Measurements at 420, 520 and 620 nm wavelengths on the spectrophotometer).
[f] Concentrated vinasse is calculated from the measurements made by dilution at the appropriate rate.

Table 2
Some properties of grape marc.

Peoperties	Value
Bulk density (g/cm^3)[a]	0.89
True density (g/cm^3)[b]	1.4974
Loss of heating at 105 °C (humidity) (%)[c]	3.1
Loss of heating at 600 °C (%)[d]	74.9
Ash (%)[e]	5.6
Potassium (%)[f]	1.74
Sodium (mg/kg)[f]	1185
Calcium (mg/kg)[f]	3500
Magnesium (mg/kg)[f]	810

[a] Weight of the grape marc, which is filled to a certain volume of container.
[b] Value found with helium pycnometer.
[c] Grape marc prepared by drying at 80 °C for 24 h at 105 °C.
[d] Grape marc dried at 80 °C, constant weighing result at 600 °C.
[e] Grape marc dried at 80 °C with constant weighing at 950 °C.
[f] By analysis of the solution obtained by dissolving the ash in 0.1 M HCl.

$$Me + oxygenatedcompounds \rightarrow Me_2O + someothercompounds$$

$$Me_2O + H_2O(g) \rightarrow 2MeOH$$

$$2Me + 2H_2O(g) \rightarrow 2MeOH + H_2\uparrow$$

During washing with water in pyrolysis, components present in the environment may result in the following reactions:

$$2Me + 2H_2O \rightarrow 2MeOH + H_2\uparrow \text{ (Me : KandNa)}$$

$$Me_2O + H_2O \rightarrow 2MeOH$$

$$Me_2CO_3 + H_2O \rightarrow MeOH + MeHCO_3$$

The post-washing strong alkali solution confirms that alkali hydroxides are present in the medium and that the above hypothetical reactions may occur. These hypothetical statements agree with the description provided by earlier studies using alkali compounds, the mechanisms of which are presented in the "General Information" section. Since active carbon and elemental alkali metal and their oxide and carbonate and hydroxides are formed, the mechanisms described by different equations occur within the same cycle.

A study focused on the carbonization of organic alkali salts (citrate, gluconate, alginate) to produce porous carbons and reported that the decomposition of organic alkali salts at relatively low temperatures (500–650 °C) resulted in alkali carbonates. The organic skeleton is also carbonized during heating. At high temperatures, alkali metal carbonates decompose to alkali metal oxides, which are then reduced to alkali metals by elemental carbon. Carbon monoxide is formed by the reaction between CO_2 and C, resulting in a microporous structure. Alkali metals contribute to the development of a different porous structure due to expansion and swelling while evaporating by entering between graphene layers. Research shows that the mechanism is transformed into a chemical activation with alkali hydroxides and alkali carbonates after alkali metal carbonates-oxides and elemental metal form (Sevilla and Fuertes, 2013; Arslanoğlu, 2019) (Fig. 3). Those studies used alkaline salts of organic acids, which are high in Me, and therefore, have greater surface areas than those in this study. In general, alkali salt/starting material is obtained by activating alkali salts with 1500 m^2/g and a large surface area due to their high ratio. Therefore, it can be stated that using a clamp as a source of potassium rather than the surface areas of active carbons with potassium compounds results in better activation.

On the other hand, the low calcium content in the water extraction solution suggested that calcium (Table 3) was converted into oxide during pyrolysis and into calcium carbonate with low solubility in alkali medium due to displacement reactions with alkali carbonates during extraction.

$$CaCO_3 \rightarrow CaO + CO_2$$

$$CaO + H_2O \rightarrow Ca^{2+} + 2OH^-$$

$$Me_2CO_3 \rightarrow 2Me^+ + CO_3^{2-} \text{ (Me : KandNa)}$$

$$HCO_3^- + OH^- \rightarrow CO_3^{2-} + H_2O$$

$$Ca^{2+} + CO_3^{2-} \rightarrow CaCO_3\downarrow$$

Thus, potassium can be extracted into a high-alkaline solution, which is essential for the precipitation of potassium-struvite, and the carbonized material surface can be of considerable value (Fig. 3).

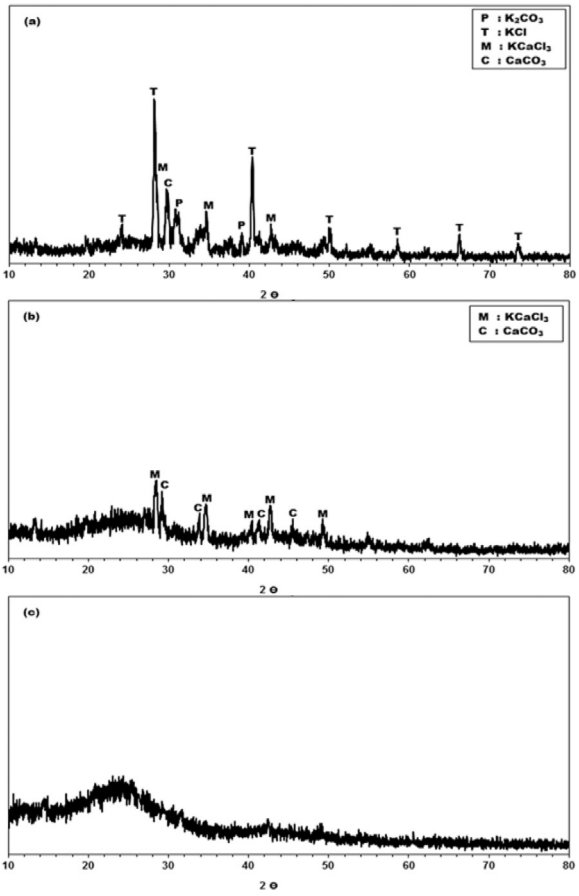

Fig. 3. V/GM: 2, pyrolysis temperature 600 °C, pyrolysis time: 120 min X-ray diffractogram of the activated carbon product obtained as a result of stabilization with pyrolysis product, water extraction residue and acid solution. (a-Pyrolysis product, b- the solid material remaining from the water extraction of the pyrolysis product, c-activated carbon obtained by stabilizing the pyrolysis product with acid solution after water extraction).

Potassium extraction values were satisfactory in all experiments. Extraction efficiency from pyrolysates at temperatures higher than 600 °C was equal to or greater than 90 %. The sodium content of the solution was equal or slightly lower. The calcium content of the solution passes to the solution at a maximum of 30 % of the initial values of the mixture. The high post-extraction Ca content of the solid residues (see EDX spectra in Fig. 4) confirms this as well. Low calcium content is ideal because calcium phosphate does not form in the solution, and therefore, K-struvite precipitation does not adversely affect product purity.

The pyrolysis temperature, which was the same in all experiments, can be increased to reduce oxidability, a measure of organic impurities. At temperatures higher than 600 °C, oxidability falls to a certain level, after which it remains more or less the same. Another indication is that the pyrolysate extracts obtained at 400 °C are yellow-brown or completely colorless, and that clear solutions emerge at temperatures higher than 600 °C. The almost-constant oxidizability at temperatures higher than 600 °C may be due to inorganic impurities, which can substantially reduce the dichromate used in the determination method, such as the chloride ion in the medium is decomposed into extraction (Table 3). As the pyrolysis temperature increased, the pH values of the extracts were about 13 or slightly more. This alkaline medium can be advantageous because it requires less alkali to reach the pH range 8–10, which is suitable for K-struvite precipitation (Arslanoglu, 2019; Arslanoglu and Tumen, 2018) (Table 3).

Table 3
Results of experiments performed at different V / GM ratio and pyrolysis temperature.

V/GM rate	Pyrolysis temperature (°C)	Pyrolysis product weight (g)	Weight of pyrolysis product after extraction with water (g)	Weight of water extraction residue after washing with acid solution (g)	Potassium in the extract (%)	Sodium in the extract (%)	Calcium in the extract (%)	COD (mg O_2/l)	Extracts pH
	400	7.20	6.29	6.05	84.1	85.1	31.9	1875	12.8
	500	6.15	5.10	4.86	83.6	80.6	27.2	947	13.4
1	**600**	5.90	4.82	4.57	89.7	81.4	18.7	446	12.8
	700	5.56	4.43	4.18	91.7	89.1	19.3	419	13.3
	800	5.26	4.07	3.82	90.0	87.8	15.6	476	13.3
	400	7.14	5.89	5.65	90.8	88.5	34.8	2315	12.8
	500	6.20	4.81	4.57	93.4	90.9	32.8	955	13.5
2	**600**	6.01	4.47	4.24	93.6	91.2	16.7	582	13.1
	700	5.49	3.92	3.69	93.1	90.4	16.0	518	13.5
	800	5.09	3.43	3.19	93.3	91.3	17.3	540	13.3
	400	7.08	5.69	5.44	88.6	89.9	36.2	3455	12.6
	500	6.17	4.57	4.33	89.3	90.5	31.2	1278	13.3
3	**600**	5.98	4.34	4.09	93.8	90.3	30.8	878	12.9
	700	5.43	3.64	3.39	92.9	90.7	26.2	816	13.3
	800	5.02	3.11	2.87	93.3	90.0	29.5	891	13.3

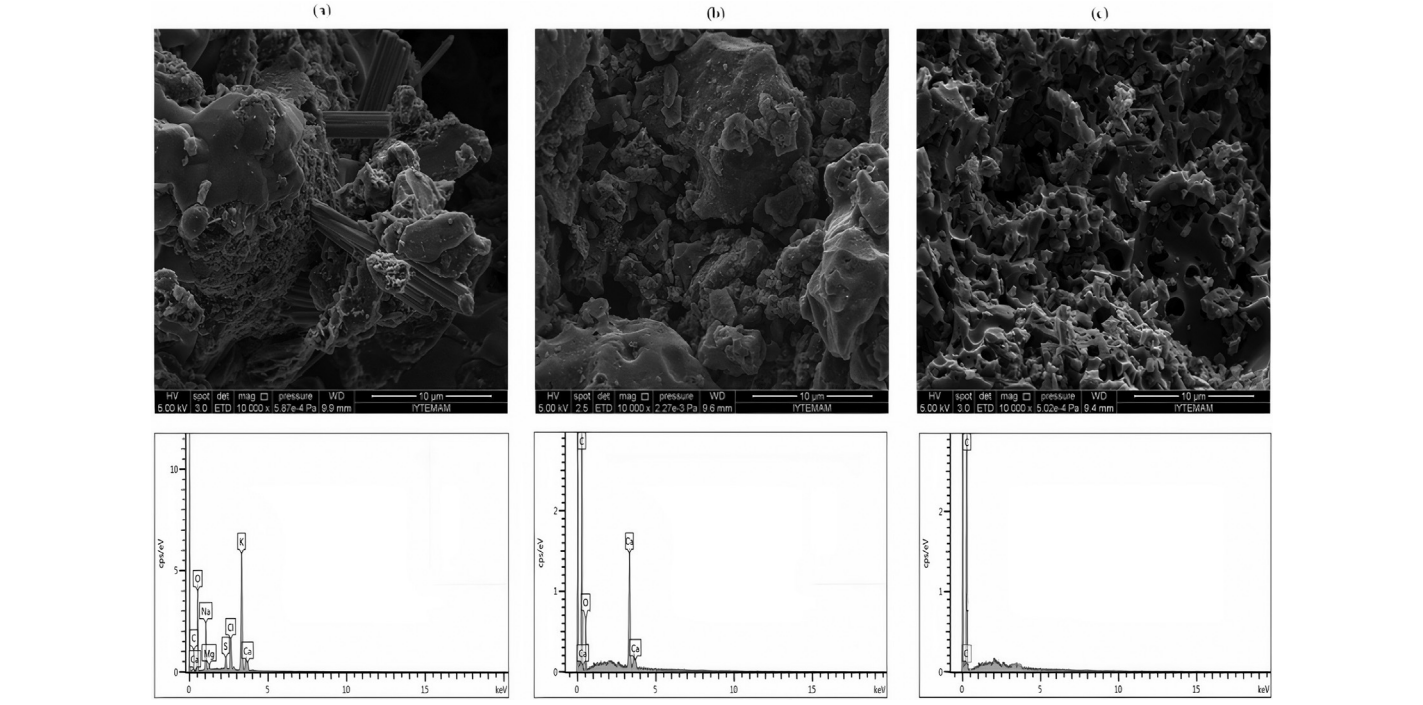

Fig. 4. SEM images and EDX spectra of the obtained activated carbon. (a-Pyrolysis product, b- the solid material remaining from the water extraction of the pyrolysis product, c-activated carbon obtained by stabilizing the pyrolysis product with acid solution after water extraction).

Tables 6 and 7 present some of the characteristics of the activated carbons obtained under the test conditions (V/GM ratio: 1, 2, and 3; pyrolysis temperature 400, 600, and 800 °C). Table 4 shows that the higher the V/GM ratio and pyrolysis temperature, the higher the specific surface areas of the carbonized products, indicating that a good activation in the form of complete carbonization and surface expansion did not occur at 400 °C. The oxidability values of the extract (Table 3) also showed that the product obtained at 400 °C was not stable for the water medium. For the V/GM ratio 3, the specific surface areas of the product after washing with acid at 800 °C were about 1000 m^2/g, which was acceptable for activated carbon. At higher temperatures, the content of the volatile substances in the active carbon was lower, the amount of fixed carbon was slightly higher, the iodine number was relatively high, and the average pore diameter was lower.

On the other hand, the higher the methylene blue and copper, the higher the products' sorption capacity. Although the number of functional groups was reduced, it yielded a more effective activated carbon using more processors at higher temperatures (Table 5). This can be attributed to the excess alkali salts in the mixture per given lignocellulosic mass, promoting activation. The activated carbons had lower pore diameters after pyrolysis at 800 °C than at 400 and 600 °C, while they had considerably high pore volumes after pyrolysis at 800 °C than at 400 °C. This might also have contributed to the relatively high sorption efficiency of the activated carbons obtained at 800 °C.

The SEM images show that washing with water and acid solution increased the specific surface areas of the pyrolysis products and that washing with acid solution resulted in a more porous structure. The increase in total pore volumes and specific surface areas also confirmed this (Fig. 4 and Table 4).

The EDX spectra of areas with possible impurity showed that washing with water resulted in a large dissolution of the pyrolysis products while washing with acid solution resulted in a substan-

Table 4
The obtained intermediate and some properties of the final carbonization product.

V/GM rate	Pyrol. Temp. (°C)	Pyrolysis product			After extraction of pyrolysis product with water			Analysis and tests for characterization of activated carbons obtained after washing of pyrolysis product with water and acid					Elemental Analysis (%)				
		Surf. Area (m^2/g)	Total pores volume (cm^3/g)	Aver. pore diamet. (Å)	Surf. Area (m^2/g)	Total pores volume (cm^3/g)	Aver. pore diamet. (Å)	Surf. Area (m^2/g)	Total pores volume (cm^3/g)	Aver. pore diamet. (Å)	*Methylene blue sorption capacity (mg/g)	**Copper sorption capacity (meş/g)	C	H	N	S	O
Grape Marc	600	2.15	0.0013	192.1	36.1	0.0172	39.1	155.2	0.0861	25.4	175.3	1.494	63.2	4.52	1.08	0.03	25.62
	800	6.91	0.0282	183.6	91.4	0.0941	29.3	315.4	0.2143	24.1	310.2	1.613	65.4	4.34	0.64	0.11	23.76
Vinasse	600	3.43	0.0236	187.2	230.8	0.1369	23.7	869.9	0.4290	20.9	382.9	1.892	67.6	2.34	3.36	0.81	20.27
	800	11.57	0.0393	172.3	952.3	0.4322	20.4	1415.6	0.7126	20.1	575.6	2.150	69.3	2.01	1.95	0.96	19.69
1	400	0.59	0.0017	112.9	9.57	0.0097	40.9	12.9	0.0147	45.6	107.9	1.354	58.8	4.11	3.39	0.10	30.56
	600	4.01	0.0119	118.8	26.45	0.0118	35.7	200.8	0.1093	21.8	196.1	1.606	61.4	2.33	3.20	0.29	28.62
	800	5.23	0.0246	119.2	647.4	0.3379	21.5	661.1	0.3472	20.9	442.5	1.921	58.4	1.56	1.87	0.40	32.41
2	400	0.75	0.0043	214.3	15.34	0.0145	39.9	15.85	0.0174	44.0	144.9	1.417	60.6	4.65	3.17	0.06	28.24
	600	3.02	0.0168	182.7	54.92	0.0526	38.4	498.4	0.2463	22.7	283.3	1.669	63.5	2.38	3.70	0.60	24.72
	800	6.04	0.0253	184.3	720.6	0.3562	20.5	997.2	0.5458	21.9	471.7	1.984	58.6	1.38	1.82	0.47	31.46
3	400	0.74	0.0027	164.1	24.72	0.0246	34.6	18.2	0.0148	32.3	169.5	1.480	60.3	4.55	4.45	0.07	27.18
	600	5.21	0.0245	189.3	62.33	0.0735	31.5	576.2	0.2587	21.0	302.1	1.732	66.8	2.54	4.26	0.79	20.05
	800	8.45	0.0301	191.4	810.4	0.3579	20.8	1075.4	0.5667	21.2	520.8	2.047	64.6	2.27	1.80	0.88	23.26

*Calculated from the analysis of the solution by shaking 0.2 g of the substance in 200 mL of 250–1000 mg l^{-1} methylen blue solution in pH 4.8 buffer medium for 24 h (Arslanoglu et al., 2009; Yaras and Arslanoğlu, 2018).
**Calculated from the analysis of the solution by shaking 1 g of the substance in 200 mL of 10 mM $CuCl_2$ solution in pH 4.8 buffer medium for 24 h (Arslanoglu et al., 2009; Yaras and Arslanoğlu, 2018).

Table 5
Some other properties of the obtained activated carbon.

V/GM rate	Pyrol. Temp. (°C)	Ash[1] (%)	Volatile Matter [2] (%)	Fixed carbon [3] (%)	pH_{zpc} [4]	Iodine Number [5] (mg/g)	Functional groups [6] (meş/g)					
							Acidic groups				Basic groups	Total
							Carboxylic	Phenolic	Lactonic	Total		
	400	3.04	39.83	57.13		19.4	1.02	0.39	0.87	2.28	0.81	3.09
1	**600**	4.16	34.35	61.49	2.75	221	0.97	0.26	0.45	1.68	0.55	2.23
	800	5.36	30.12	64.52		590	0.74	0.28	0.41	1.43	0.38	1.81
	400	3.28	31.91	64.81		31.6	1.34	0.47	0.66	2.47	0.96	3.43
2	**600**	5.10	28.70	66.20	3.05	433	1.13	0.30	0.39	1.82	0.72	2.54
	800	6.27	25.34	68.39		881	0.61	0.25	0.52	1.38	0.61	1.99
	400	3.45	27.91	68.64		27.2	1.28	0.39	0.73	2.40	1.08	3.48
3	**600**	5.56	25.58	68.86	3.90	513	0.97	0.34	0.39	1.70	0.74	2.44
	800	7.19	22.54	69.27		968	0.65	0.30	0.27	1.22	0.89	2.11

[1] Ash determination: according to ASTM D 2866-94.
[2] Determination of volatile matter: Made according to ASTM D 5832-98.
[3] Determination of fixed carbon: It was found by subtracting the sum of ash and volatile matter from 100.
[4] Determination of pHzpc: It was made by balancing the active carbons in NaCl solutions at different pHs and measuring the pH in the final mixtures (Órfão et al., 2006; Rivera-Utrilla et al., 2001).
[5] Determination of iodine number: According to ASTM D 4607.
[6] Determination of functional groups: Boehm titration was performed according to the method (Boehm, 1994, 2002).

tial dissolution of the inorganics. The calcium peaks in some of the EDX diagrams solid residues obtained by extracting pyrolysis products with water supported the hypothesis that $CaCO_3$ forms on the surface during extraction. An acid solution was used to remove those impurities. EDX analysis provides information in that regard (Fig. 4). According to the results, the average pore diameter of the activated carbon obtained by increasing the pyrolysis time to 120 min remained almost constant, while the specific surface and total pore volume increased and then remained constant for a long time. Oxidability also decreased with an increase in the pyrolysis time. The oxidability value of 600 mg-O_2/L suggested that a 120 min pyrolysis at 600 °C was suitable for potassium extraction and low impurities.

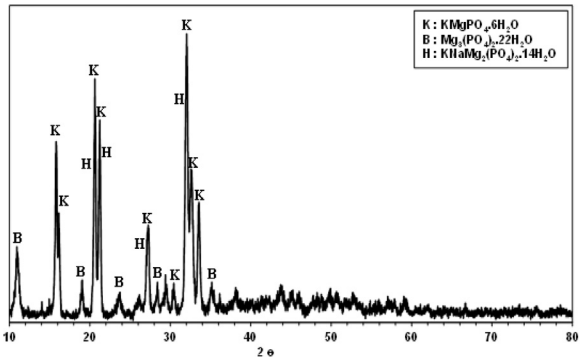

Fig. 5. X-ray diffractogram of potassium-struvite containing product precipitated at pH 9.5 with a K: Mg: P ratio of 1: 1: 1.

4.3. Obtaining potassium-struvite

The extract obtained in the first extraction step was used as a resolvent to obtain a potassium-containing solution at the end of the two-step extraction process (Fig. S2). A portion of the solution was evaporated to a potassium concentration of 2 M. The potassium-containing solutions were referred to as the "extract" and "concentrated extract," respectively. Tables S3 and S4 show the compositions of the extract and the concentrated extract, respectively. Potassium-struvite precipitation was obtained from the extract according to Fig. S3.

Table 6 shows the results of changing the K: Mg: P ratios and the pH at 9.5, indicating that the higher the Mg and P ratios, the higher the precipitated potassium content but lowered the potassium content in the product (Arslanoglu and Tumen, 2018). This is understood by the fact that the amount of the product increased with a particular solution containing the same amount of potassium. In addition to potassium-struvite, various magnesium phosphates precipitated, increasing the amount of the product and reducing potassium concentration. The presence of the tertiary magnesium phosphate compound $Mg_3(PO_4)_2.22H_2O$ (cattiite) in the XRD images confirmed this.

Extract (250 mL), K, Mg, and P (ratio of 1: 1: 1), final potassium (about 16 g/L), water (100 mL), and NaOH solution (about ten g/L) with a pH of 9.5 were used in the experiments, and no Na_3PO_4 crystallization was observed. The amount of the extract and reagent remained the same. However, more water was added to reduce the final potassium concentration to about 5 g/L, and no significant difference was observed in the amount of the precipitate. About 50.4 % of potassium was recovered in one experiment. In another one, more water was added to reduce the potassium concentration to 2 g/L, resulting in a 36.65 % potassium yield. It is reported that potassium yield decreases from 85 % to 72 % when the K, Mg, and P have a ratio of 1: 2: 2 with a pH of 10, and when reagents (from 100 mM to 25 mM) are added to the mixture of potassium (Kuşçuoğlu, 2008). Other studies report that potassium yield decreases in more dilute systems. Of course, precipitation can be carried out in the most concentrated medium possible in terms of the amount, properties, and re-use of residual solutions or the challenges of waste treatment.

In this study, necessary reagents were used in the experiments performed at about 9.5 pH with the K: Mg: P ratio of 1: 1: 1 in order to obtain a slow-release fertilizer. Figs. 5–6 and Figs. S4-S6 present the XRD and FTIR diagrams, TG/DTA thermogram, particle size distribution graph and SEM-EDX image, and spectrum of the product, respectively. The XRD diagram showed that potassium-struvite formed (Fig. 5), indicating that potassium-struvite formation was more efficient in an alkaline medium, which is consistent with the literature (Rahman et al., 2014; Liu et al., 2013; Xu et al., 2011).

The FTIR spectra for potassium-struvite were similar to those reported by earlier studies (Kiani et al., 2019; Lustosa Filho et al., 2019). The broadband of 3300−2600 cm^{-1} of the product spectrum coincided with the basic stress mode of crystal water molecules in many inorganic hydrated compounds. The weaker band crystallization of about 2300 cm^{-1} can be attributed to the tensile vibration of a set of water molecules H-O-H. It is reported that the band in that area is due to the hydrogen bond between water and phos-

Table 6
Results of potassium struvite precipitation experiments (Experiments were performed according to Fig. S3) [Precipitations were carried out at pH 9.5, room temperature (23-27 °C) and 6 h complete].

Exp. No.	pH_i	K:Mg:P rate			Final pH in precipitation	Obtained product (Dried at 40 °C)	Product composition					K recovery (%)
		K	Mg	P			K_2O (%)	MgO (%)	P_2O_5 (%)	Na_2O (%)	LI* (%)	
1	9.42	1	1	1	9.27	23.18	10.67	17.63	31.88	3.21	39.03	50.40
2	9.51	1.5	1	1	9.36	13.68	11.11	19.82	35.76	2.28	30.12	30.96
3	9.55	2	1	1	9.41	10.74	12.27	18.91	34.39	1.17	31.26	26.87
4	9.39	1	1	1.5	9.22	23.67	8.05	17.26	35.14	3.57	38.78	38.83
5	9.44	1.5	1	1.5	9.30	16.07	9.07	17.15	34.56	3.68	38.69	29.71
6	9.52	2	1	1.5	9.41	11.37	10.09	17.73	36.67	2.51	32.04	23.37
7	9.38	1	1	2	9.20	23.62	7.61	16.97	31.06	3.57	43.10	36.65
8	9.57	1.5	1	2	9.45	15.94	7.76	16.80	30.48	3.45	42.96	25.21
9	9.45	2	1	2	9.29	12.12	7.90	16.76	30.05	3.39	40.80	19.53
10	9.53	1	1.5	1	9.35	18.56	4.99	25.10	39.56	1.58	31.34	18.89
11	9.42	1.5	1.5	1	9.20	13.85	5.28	22.59	35.19	0.87	37.25	14.92
12	9.59	2	1.5	1	9.38	9.50	4.99	24.38	38.61	0.37	35.02	9.67
13	9.47	1	2	1	9.35	19.98	2.23	20.80	36.72	1.35	36.95	9.08
14	9.50	1.5	2	1	9.32	12.61	2.52	21.81	38.86	0.77	37.29	6.48
15	9.53	2	2	1	9.41	9.41	2.64	22.11	39.27	0.32	34.41	5.06
16	9.45	1	1.5	1.5	9.30	35.61	8.63	17.35	31.18	3.45	43.26	62.65
17	9.49	2	1.5	1.5	9.31	17.05	11.11	18.22	32.54	3.45	35.87	38.59
18	9.53	1	2	2	9.27	45.73	8.78	18.16	32.19	3.33	39.74	81.81
19	9.39	1.5	2	2	9.25	31.48	9.07	17.45	31.37	3.10	40.86	58.18
20	9.48	1	3	3	9.23	61.50	7.15	20.15	36.49	3.21	38.75	89.56

* Loss on ignition, At a temperature of 400 °C where the crystal water is completely removed.

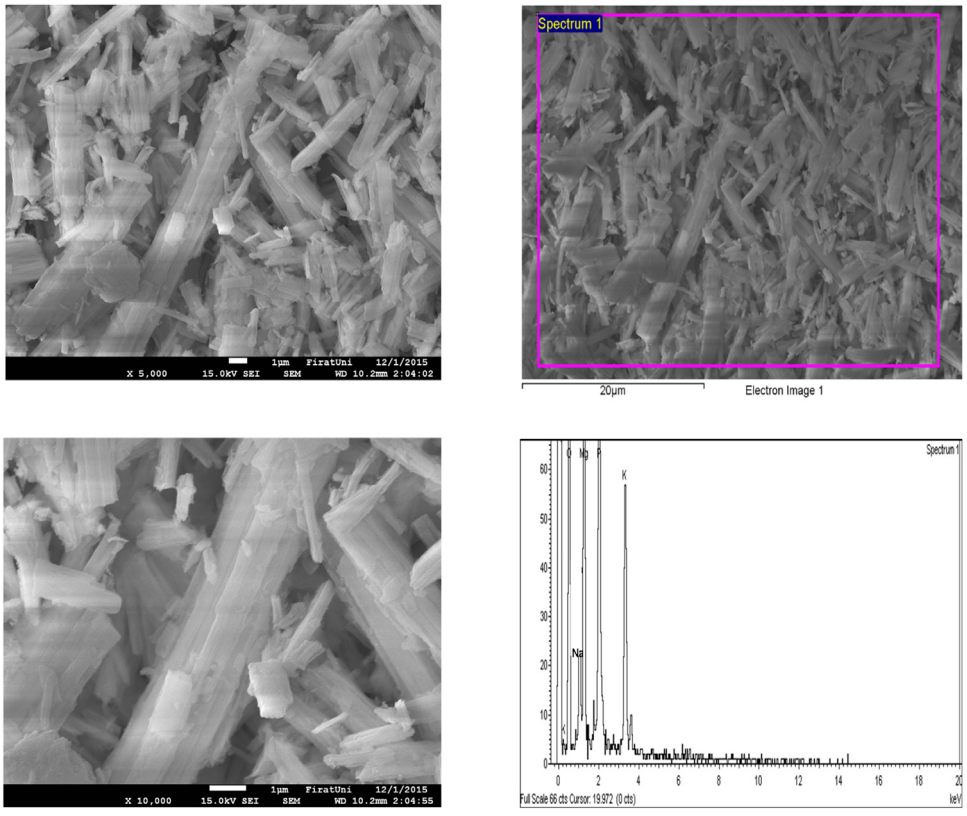

Fig. 6. SEM-EDX images of potassium-struvite-containing product precipitated at pH 9.5 with a K: Mg: P ratio of 1: 1: 1.

phate and that modes of bending at medium intensity band H-O-H vibrations at 1600 cm^{-1} is due to the deformation of the ν_2 H-O-H water molecule (Kiani et al., 2019).

Free phosphate ion has four normal modes of vibration: ν_1, ν_2, ν_3, and ν_4, ν_1 and ν_3 are stress and bending vibrations of ν_2 and ν_4, and only ν_3 (asymmetric stress vibration) and ν_4 (asymmetric bending vibration) are infrared active (Lustosa Filho et al., 2019). According to the FTIR spectrum, the strong peaks of 1000 cm^{-1} correspond to ν_3 asymmetric tensile vibrations, and the asymmetric band at 570 cm^{-1} conforms to ν_4. This interpretation is provided by (Lustosa Filho et al., 2019). Chauhan et al. (Chauhan et al. (2011)) and Stefov et al. (Stefov et al. (2004)) attribute the band around 430 cm^{-1} to ν_2 mode or Mg or O tensile vibration. They also state that the absorption at 740 cm^{-1} is due to the Mg-O bond. In our samples, these two bands were observed at approximately 420 cm^{-1} and 730 cm^{-1} (Fig. S4).

Table 7
Results of solubility tests of potassium-struvite containing product in various media.

Solvents	Initial pH of solvents	pH_f	Experimental dissolution	
			K_2O %	P_2O_5 %
Water	6.84	9.18	2.17	0.77
Tap water*	7.52	9.56	2.57	0.65
0.001 M HCl	3.27	8.41	10.03	11.16
0.001 M Citric acid	3.56	8.64	12.29	10.53
0.001 M Acetic acid	3.89	9.01	7.23	6.21
0.001 M Formic acid	3.04	8.60	10.65	9.65
0.001 M Sodium Humate	8.25	9.26	3.47	3.86
0.001 M Oxalic acid	3.77	8.92	9.24	9.51
0.001 M Ammonium citrate	5.53	8.76	6.89	6.12
0.001 M Ammonium oxalate	6.27	9.71	5.96	6.56
0.001 M Ammonium acetate	6.73	9.25	5.14	4.85
0.001 M DTPA	3.64	8.89	14.94	16.40
0.001 M Na_2-EDTA	5.21	9.12	14.15	13.90

* Hardness 320 mg-$CaCO_3$ / L.

Fig. 6 shows the SEM-EDX spectra at 5000 and 10,000 magnifications, indicating high potassium-struvite content in the samples and particles in the rod structure. The high potassium content confirmed that the structures were potassium-struvite. The product had a small particle size (Fig. S5). 6-h, 24-h, and 120-h precipitation experiments yielded approximately 16μ, 20μ, and 28μ of particle size, respectively. This result suggests that if the NaOH solution is used to adjust pH, then the average particle size of a precipitated product is low. Fig. S6 shows the TG/DTA diagram of the solid product, which is consistent with the literature (Rahman et al., 2014; Liu et al., 2013; Xu et al., 2011). The apparent density and true density and the BET specific surface area of the samples were 0.845, 1.8739 g/cm^3, 65.4 m^2/g, respectively, (Arslanoglu, 2019; Arslanoglu and Tumen, 2018).

4.4. Potassium struvite solubility

The dissolution rates of potassium and phosphorus in distilled and tap water at a solid-liquid ratio (10 g/L) were 2.17 % and 0.77 %, respectively (Table 7), which were higher than those reported by (Salutsky and Steiger, 1964). This might be because our product was not pure potassium-struvite and possibly contained magnesium phosphates and perhaps had a small particulate structure. Salutsky and Steiger (Salutsky and Steiger, 1964) have shown that potassium-struvite dissolves in water to disproportionation, resulting in magnesium phosphate.

Tests using mineral acid, organic acids, and compounds of various phosphate fertilizers have been proposed for solubility (Chen et al., 2018; Bandyopadhyay et al., 2008; Chandra et al., 2009). This study focused on various organic acids and their compounds secreted by plant roots and determined that those substances dissolved in the solution (Table 7). Table 7 shows that potassium and phosphate dissolution rates were different, given the stoichiometric formula of the potassium-struvite. This might be because the structure was not only potassium-struvite but also contained some other magnesium phosphates. Table 7 also shows that the dissolution rate was 14.94 %, 14.15 %, and 12.29 % in DTPA, Na_2-EDTA, and citric acid solutions, respectively. Considering the solution rate, contact time, and solid/liquid ratio, we can state that the product was a slow-release fertilizer. According to Trenkel (Rech et al., 2019), 1-day dissolution of a slow-release fertilizer should be characteristically below 15 % at 25 °C, in case of prolonged contact with water. In our study, 10 g of solids were contacted by stirring in one liter of distilled water for one day and then filtered. Afterward, the solid was dried and weighed at 40 °C. The resulting dissolution rate was about 0.75 %, indicating that it dissolved much more slowly than reported by Trenkel (Rech et al., 2019).

5. Conclusion

This study proposed a process to obtain a slow-release potassium magnesium phosphate fertilizer from a mixture of vinasse (a by-product of the sugar or ethanol industry) and grape marc (a by-product of the wine-making industry). The following three main results have been obtained with the products obtained.

- The first step of the study shows that when a mixture of a significant amount of potassium-containing vinasse and a small amount of potassium-containing grape marc is pyrolyzed and extracted with water, potassium is dissolved in solution with a high degree of extraction. Thus, potassium complex is obtained from a complex to a clean environment, which is essential for potassium-struvite precipitation (high in alkalinity), as calcium-free as possible. The results also show that the potassium in the mixture causes activation, resulting in an activated carbon as a by-product of pyrolysis.
- The second step shows that precipitation with NaOH solution is suitable for product yield and purity and that the total concentration is not too much to result in sodium phosphate crystallization. Mg and P can be increased to deposit potassium at a high rate. Although our product has a lower potassium concentration, different types of products can be obtained by identifying suitable conditions with a high transfer rate of potassium to the precipitate. However, the value of a mixed product (as a fertilizer) with potassium struvite and magnesium phosphate should be separately determined.
- The third step shows that the solubility of the product is 0.75 % in the 24-h precipitation experiment and that the solubility based on potassium is approximately 2%. These values indicate that the product is an efficient slow-release fertilizer.

Declaration of Competing Interest

The authors declare that there are no conflicts of interest regarding the publication of this paper.

Acknowledgments

This study was financially supported by the Scientific and Technological Research Council of Turkey (TUBITAK) (Project No: 113M250). The authors would like to thank Semih Kaya, Pınar Akbayır, and Ufuk Tarhan for their assistance in the experiments.

Appendix A. Supplementary data

Supplementary material related to this article can be found, in the online version, at doi:https://doi.org/10.1016/j.psep.2021.01.025.

References

Alcañiz-Monge, J., Illán-Gómez, M.J., 2008. Insight into hydroxides-activated coals: chemical or physical activation? J. Colloid Interface Sci. 318 (1), 35–41.

Algieri, A., Andiloro, S., Tamburino, V., Zema, D.A., 2019. The potential of agricultural residues for energy production in Calabria (Southern Italy). Renew. Sustain. Energy Rev. 104, 1–14.

Arslanoğlu, H., 2016. Development of a Process for Producing Slow Released Potassium-struvite Fertilizer from Vinasse and Grape Marc. PhD Thesis. Firat University, Turkey, Elazığ (In Turkish).

Arslanoğlu, H., 2019. Direct and facile synthesis of highly porous low cost carbon from potassium-rich wine stone and their application for high-performance removal. J. Hazard. Mater. 374, 238–247.

Arslanoglu, H., 2019. Adsorption of micronutrient metal ion onto struvite to prepare slow release multielement fertilizer: copper (II) doped-struvite. Chemosphere 217, 393–401.

Arslanoglu, H., Tumen, F., 2018. Cd and nutrient elements release into various aqueous solutions from synthesized K-struvite fertilizer. Commun. Soil Sci. Plant Anal. 49 (17), 2175–2188.

Arslanoglu, H., Altundogan, H.S., Tumen, F., 2009. Heavy metals binding properties of esterified lemon. J. Hazard. Mater. 164 (2–3), 1406–1413.

Arslanoğlu, H., Kaya, S., Tümen, F., 2020. Cr (VI) adsorption on low-cost activated carbon developed from grape marc-vinasse mixture. Part. Sci. Technol. 38 (6), 768–781.

Bandyopadhyay, S., Bhattacharya, I., Ghosh, K., Varadachari, C., 2008. New slow-releasing molybdenum fertilizer. J. Agric. Food Chem. 56 (4), 1343–1349.

Barampouti, E.M., Mai, S., Malamis, D., Moustakas, K., Loizidou, M., 2019. Liquid biofuels from the organic fraction of municipal solid waste: a review. Renew. Sustain. Energy Rev. 110, 298–314.

Boehm, H.P., 1994. Some aspects of the surface chemistry of carbon blacks and other carbons. Carbon 32 (5), 759–769.

Boehm, H.P., 2002. Surface oxides on carbon and their analysis: a critical assessment. Carbon 40 (2), 145–149.

Chandra, T.C., Mirna, M.M., Sunarso, J., Sudaryanto, Y., Ismadji, S., 2009. Activated carbon from durian shell: preparation and characterization. J Taiwan Inst.Chem. Eng. 40 (4), 457–462.

Chauhan, C.K., Vyas, P.M., Joshi, M.J., 2011. Growth and characterization of Struvite-K crystals. Cryst. Res. Technol. 46 (2), 187–194.

Chen, M., Li, Z., Huang, P., Li, X., Qu, J., Yuan, W., Zhang, Q., 2018. Mechanochemical transformation of apatite to phosphoric slow-release fertilizer and soluble phosphate. Process Saf. Environ. Prot. 114, 91–96.

Chojnacka, K., Gorazda, K., Witek-Krowiak, A., Moustakas, K., 2019. Recovery of fertilizer nutrients from materials-contradictions, mistakes and future trends. Renew. Sustain. Energy Rev. 110, 485–498.

Ferjani, A.I., Jeguirim, M., Jellali, S., Limousy, L., Courson, C., Akrout, H., Bennici, S., 2019. The use of exhausted grape marc to produce biofuels and biofertilizers: effect of pyrolysis temperatures on biochars properties. Renew. Sustain. Energy Rev. 107, 425–433.

Hidalgo, D., Martín-Marroquín, J.M., Corona, F., 2019. A multi-waste management concept as a basis towards a circular economy model. Renew. Sustain. Energy Rev. 111, 481–489.

Irfan, S.A., Razali, R., KuShaari, K., Mansor, N., Azeem, B., Versypt, A.N.F., 2018. A review of mathematical modeling and simulation of controlled-release fertilizers. J. Control. Release 271, 45–54.

Kiani, D., Silva, M., Sheng, Y., Baltrusaitis, J., 2019. Experimental insights into the genesis and growth of struvite particles on low-solubility dolomite mineral surfaces. J. Physic. Chem. 123 (41), 25135–25145.

Kuşçuoğlu, S., 2008. Determination of K-struvite Precipitation Aplication. Master Thesis. Istanbul Technical University, Institute of Science and Technology, pp. 59 (In Turkish).

Lafka, T.I., Sinanoglou, V., Lazos, E.S., 2007. On the extraction and antioxidant activity of phenolic compounds from winery wastes. Food Chem. 104 (3), 1206–1214.

Li, X., Mupondwa, E., 2018. Commercial feasibility of an integrated closed-loop ethanol-feedlot-biodigester system based on triticale feedstock in Canadian Prairies. Renew. Sustain. Energy Rev. 97, 401–413.

Liang, Y., Zhao, X., Strait, M., Wen, Z., 2012. Use of dry-milling derived thin stillage for producing eicosapentaenoic acid (EPA) by the fungus Pythium irregulare. Bioresour. Technol. 111, 404–409.

Lide, D.R., 1995. CRC Handbook of Chemistry and Physics: A Ready-Reference Book of Chemical and Physical Data, 72nd ed. CRC press, Boca Raton, pp. 4–89.

Liu, Y., Kumar, S., Kwag, J.H., Ra, C., 2013. Magnesium ammonium phosphate formation, recovery and its application as valuable resources: a review. J. Chem. Technol. Biotech. 88 (2), 181–189.

Lustosa Filho, J.F., Barbosa, C.F., da Silva Carneiro, J.S., Melo, L.C.A., 2019. Diffusion and phosphorus solubility of biochar-based fertilizer: visualization, chemical assessment and availability to plants. Soil Tillage Res. 194, 104298.

Órfão, J.J.M., Silva, A.I.M., Pereira, J.C.V., Barata, S.A., Fonseca, I.M., Faria, P.C.C., Pereira, M.F.R., 2006. Adsorption of a reactive dye on chemically modified activated carbons—influence of pH. J. Colloid Interface Sci. 296 (2), 480–489.

Patti, A.F., Issa, G.J., Smernik, R., Wilkinson, K., 2009. Chemical composition of composted grape marc. Water Sci. Technol. 60 (5), 1265–1271.

Rahman, M.M., Salleh, M.A.M., Rashid, U., Ahsan, A., Hossain, M.M., Ra, C.S., 2014. Production of slow release crystal fertilizer from wastewaters through struvite crystallization–a review. Arabian J. Chem. 7 (1), 139–155.

Rech, I., Withers, P.J., Jones, D.L., Pavinato, P.S., 2019. Solubility, diffusion and crop uptake of phosphorus in three different struvites. Sustainability 11 (1), 134.

Reis, C.E.R., Carvalho, A.K.F., Bento, H.B., de Castro, H.F., 2019. Integration of microbial biodiesel and bioethanol industries through utilization of vinasse as substrate for oleaginous fungi. Bioresour. Technol. Rep. 6, 46–53.

Rivera-Utrilla, J., Bautista-Toledo, I., Ferro-García, M.A., Moreno-Castilla, C., 2001. Activated carbon surface modifications by adsorption of bacteria and their effect on aqueous lead adsorption. J. Chem. Technol. Biotech. 76 (12), 1209–1215.

Salutsky, M.L., Steiger, R.P., 1964. Properties of fertilizer materials, metal potassium phosphates. J. Agric. Food Chem. 12 (6), 486–491.

Sevilla, M., Fuertes, A.B., 2013. A general and facile synthesis strategy towards highly porous carbons: carbonization of organic salts. J. Mater. Chem. A 1 (44), 13738–13741.

Stefov, V., Soptrajanov, B., Spirovski, F., Kuzmanovski, I., Lutz, H.D., Engelen, B., 2004. Infrared and Raman spectra of magnesium ammonium phosphate hexahydrate (struvite) and its isomorphous analogues. I. Spectra of protiated and partially deuterated magnesium potassium phosphate hexahydrate. J. Mol. Struc. 689 (1-2), 1–10.

Tian, D., Li, Z., O'Connor, D., Shen, Z., 2020. The need to prioritize sustainable phosphate-based fertilizers. Soil Use Manage. 36 (3), 351–354.

Tümen, F., 2016. Development of a Process for Producing Slow Released Potassium-struvite Fertilizer from Vinasse and Grape Marc. TUBITAK Project No: 113M250 (In Turkish).

Xu, K., Wang, C., Liu, H., Qian, Y., 2011. Simultaneous removal of phosphorus and potassium from synthetic urine through the precipitation of magnesium potassium phosphate hexahydrate. Chemosphere 84 (2), 207–212.

Yang, Y., Liu, J., Wang, B., Liu, R., Zhang, T., 2019. A thermodynamic modeling approach for solubility product from struvite-k. Comput. Mater. Sci. 157, 51–59.

Yaras, A., Arslanoğlu, H., 2018. Valorization of paper mill sludge as adsorbent in adsorption process of copper (II) ion from synthetic solution: kinetic, isotherm and thermodynamic studies. Arabian J. Sci. Eng. 43 (5), 2393–2402.